Int. J. Heat Mass Transfer. Vol. 23, pp. 1573–1580
Pergamon Press Ltd. 1980. Printed in Great Britain

CRITICAL HEAT FLUX OF FORCED CONVECTION BOILING IN UNIFORMLY HEATED VERTICAL TUBES (CORRELATION OF CHF IN HP-REGIME AND DETERMINATION OF CHF-REGIME MAP)

Y. KATTO
Department of Mechanical Engineering, University of Tokyo,
Hongo, Bunkyo-ku, Tokyo, Japan

(*Received* 23 *January* 1980)

Abstract—Being faced with two important questions arising from the author's previous studies of generalized correlation of critical heat flux (CHF) in tubes, experimental data of CHF obtained in HP-regime (that is, high pressure regime) are re-examined to obtain new equations for correlating CHF in this regime with higher accuracy. Then, the criterion for the onset of CHF in HP-regime can also be revised so as to satisfy all the existing experimental data, and finally a clearly defined map of characteristic regimes of CHF in uniformly heated tubes is determined.

NOMENCLATURE

- C, constant, equation (4);
- d, I.D. of heated tube [m];
- G, mass velocity [$\mathrm{kgm^{-2}s^{-1}}$];
- H_{fg}, latent heat of evaporation [$\mathrm{Jkg^{-1}}$];
- ΔH_i, enthalpy of inlet subcooling [$\mathrm{Jkg^{-1}}$];
- K, parameter for the effect of inlet subcooling, equation (1);
- l, length of heated tube [m];
- p, absolute pressure [bar];
- q_c, critical heat flux [$\mathrm{Wm^{-2}}$];
- q_{co}, q_c for $\Delta H_i = 0$ [$\mathrm{Wm^{-2}}$].

Greek symbols

- ρ_l, density of liquid [$\mathrm{kgm^{-3}}$];
- ρ_v, density of vapor [$\mathrm{kgm^{-3}}$];
- σ, surface tension [$\mathrm{Nm^{-1}}$].

1. INTRODUCTION

RECENTLY, the author has made a series of studies [1–4] of generalized equations for correlating experimental data of critical heat flux (CHF) of forced convection boiling in uniformly heated vertical tubes, in which the critical heat flux q_c is expressed as

$$q_c = q_{co}\left(1 + K\frac{\Delta H_i}{H_{fg}}\right) \tag{1}$$

where ΔH_i is the enthalpy of inlet subcooling, and q_{co} (i.e. q_c for $\Delta H_i = 0$) is given in the following generalized form:

$$\frac{q_{co}}{GH_{fg}} = f\left(\frac{\rho_v}{\rho_l}, \frac{\sigma\rho_l}{G^2 l}, \frac{l}{d}\right). \tag{2}$$

In the above correlation, four characteristic regimes are classified, namely L-regime (the regime presumably corresponding to the so-called dryout), N-regime (the regime presumably corresponding to the so-called DNB), H-regime (the intermediate regime between L- and N-regime), and HP-regime (the regime which appears in place of N-regime at high pressure). Then, in all the regimes except N-regime, the linear q_c–ΔH_i relationship such as mentioned in Collier's book [5] holds, so that the dimensionless parameter K on the RHS of equation (1) is determined independently of $\Delta H_i/H_{fg}$.

As for the above-mentioned studies, however, it must be remembered that two important questions remain unsolved regarding HP-regime. First, according to [3], predictions of the parameter K derived theoretically from equation (2) show a small but regular deviation from experimental data in HP-regime, suggesting that the generalized correlation equation of q_{co} given by the author for HP-regime is somewhat defective. Second, according to [4], the criterion for the onset of HP-regime given by the author tentatively agrees with the trend of experimental data, but some quantitative discrepancies are clearly observed. In this paper, therefore, a study is made to solve these questions of HP-regime, and at the same time, to give a CHF-regime map free of such ambiguities as seen in the author's previous studies.

2. SUMMARY OF CORRELATION EQUATIONS OF CHF PROPOSED SO FAR

Correlation equations of CHF proposed through the author's previous studies [1–4] are summarized as in the following.

2.1. *Generalized correlation equations of* q_{co}

Correlation of q_{co} based on equation (2) are illustrated in Fig. 1, where two typical cases of $l/d = 50$ and 200 are shown for $\rho_v/\rho_l = 0.01787$ and 0.3216 (which correspond to $p = 29.5$ and 196 bar respectively in case

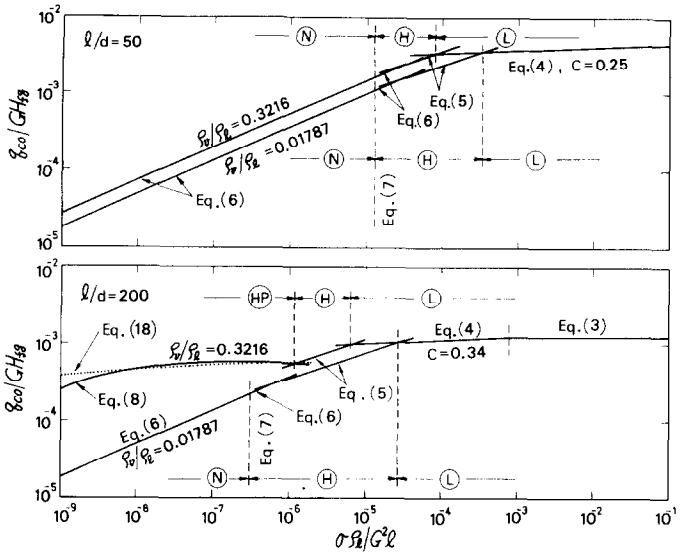

FIG. 1. Examples of the prediction by the author's generalized correlation equations of q_{co}. (L): L-regime, (H): H-regime, (N). N-regime and (HP): HP-regime.

of water), and the equations noted in Fig. 1 are as follows.

L-regime:

$$\frac{q_{co}}{GH_{fg}} = \frac{0.25}{l/d} \tag{3}$$

and

$$\frac{q_{co}}{GH_{fg}} = C\left(\frac{\sigma\rho_l}{G^2 l}\right)^{0.043}\frac{1}{l/d} \tag{4}$$

where $C = 0.25$ for $l/d < 50$, $C = 0.34$ for $l/d > 150$, and C changes with l/d in the range of $l/d = 50$–150.

H- and N-regime:

$$\frac{q_{co}}{GH_{fg}} = 0.10\left(\frac{\rho_v}{\rho_l}\right)^{0.133}\left(\frac{\sigma\rho_l}{G^2 l}\right)^{1/3}\frac{1}{1+0.0031\,l/d} \tag{5}$$

and

$$\frac{q_{co}}{GH_{fg}} = 0.098\left(\frac{\rho_v}{\rho_l}\right)^{0.133}\left(\frac{\sigma\rho_l}{G^2 l}\right)^{0.433} \times \frac{(l/d)^{0.27}}{1+0.0031\,l/d}, \tag{6}$$

and the boundary between H- and N-regime is given by

$$\frac{\sigma\rho_l}{G^2 l} = \left(\frac{0.77}{l/d}\right)^{2.70}, \quad \text{or} \quad \frac{l}{d} = \frac{0.77}{(\sigma\rho_l/G^2 l)^{0.37}}. \tag{7}$$

HP-regime:

$$\frac{q_{co}}{GH_{fg}} = 8.20\left(\frac{\rho_v}{\rho_l}\right)^{0.65}\left(\frac{\sigma\rho_l}{G^2 l}\right)^{0.453} \times \frac{1}{1+107(\sigma\rho_l/G^2 l)^{0.54}\,l/d}. \tag{8}$$

2.2. *Predictions of K*

Predictions of K which are derived theoretically from the generalized correlation equations of q_{co} for L-, H- and HP-regime are as follows [3].

K for L-regime: K_L

From equation (4),

$$K_L = \frac{1.043}{4C(\sigma\rho_l/G^2 l)^{0.043}} \tag{9}$$

K for H-regime: K_H

From equation (5),

$$K_H = \frac{5}{6}\frac{0.0124 + d/l}{(\rho_v/\rho_l)^{0.133}(\sigma\rho_l/G^2 l)^{1/3}} \tag{10}$$

and from equation (6),

$$K_H = 0.416\frac{(0.0221 + d/l)(d/l)^{0.27}}{(\rho_v/\rho_l)^{0.133}(\sigma\rho_l/G^2 l)^{0.433}} \tag{11}$$

K for HP-regime: K_{HP}

From equation (8),

$$K_{HP} = 0.0138\frac{215(\sigma\rho_l/G^2 l)^{0.54} + d/l}{(\rho_v/\rho_l)^{0.65}(\sigma\rho_l/G^2 l)^{0.453}}. \tag{12}$$

3. DETAILS OF THE QUESTIONS RELATED TO HP-REGIME

3.1. *The first question*

Figure 2 is the comparison of K_{HP} predicted by equation (12) with the experimental data of K_{HP} collected in Fig. 18 of [1], showing a regular deviation between the predicted and experimental K_{HP}. In the paper [3], however, owing to the apparent high accuracy of equation (8) as compared with experimen-

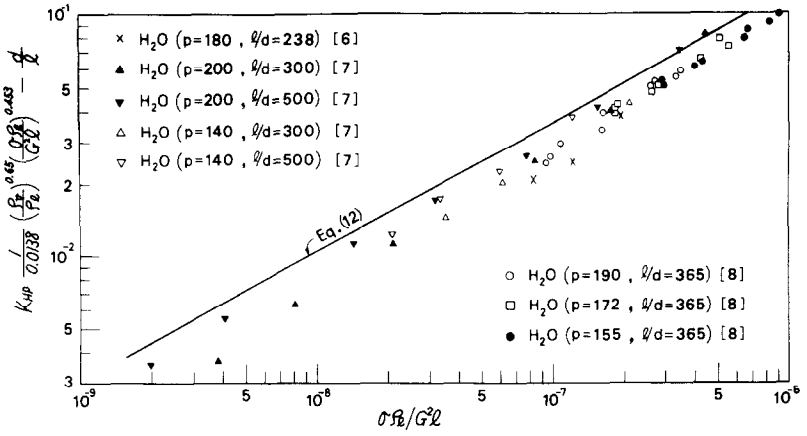

FIG. 2. Comparison between prediction of equation (12) and experimental data for K_{HP}.

tal data of q_{co} (see Fig. 12 of [1]), the cause of the above-mentioned deviation of K_{HP} was regarded as unknown.

3.2. *The second question*

As shown in [3], the boundary between L- and H-regime can be determined by eliminating q_{co} from equations (4) and (5) as follows:

$$\frac{l}{d} = \frac{1}{(0.10/C)(\rho_v/\rho_l)^{0.133}(\sigma\rho_l/G^2l)^{0.29} - 0.0031}. \quad (13)$$

Next, as shown in [1], q_{co} is eliminated from equations (5) and (6) in H-regime to give the boundary between the realms of these two equations as:

$$\frac{l}{d} = \frac{1.077}{(\sigma\rho_l/G^2l)^{0.37}}. \quad (14)$$

In addition, as shown in [1], the boundary between H- and N-regime is given by equation (7), and the boundary between H- and HP-regime is determined by eliminating q_{co} from equations (5) and (8) as follows:

$$\frac{l}{d} = \frac{82(\rho_v/\rho_l)^{0.517} - (\sigma\rho_l/G^2l)^{-0.12}}{107(\sigma\rho_l/G^2l)^{0.42} - 0.254(\rho_v/\rho_l)^{0.517}}. \quad (15)$$

Then, Fig. 3 shows two different examples of CHF-regime map made with equations (7), (13) to (15) for the case of $\rho_v/\rho_l = 0.3216$, where C on the RHS of equation (13) is assumed to change from 0.25 to 0.34 linearly with l/d in the range of $l/d = 50$ to 150.* First, in case of Fig. 3(A), a horizontal line passing through the intersecting point P′ of equations (15) and (7) is assumed to separate HP- and N-regime, and this is the idea adopted in [1, 2]. In this case, therefore, the relation between ρ_v/ρ_l and l/d at the point P′ is obtained by eliminating $\sigma\rho_l/G^2l$ from equations (15) and (7) as follows:

$$\frac{\rho_v}{\rho_l} = \left\{\frac{79.5(l/d)^{-0.134} + 1.08(l/d)^{0.324}}{0.254(l/d) + 82}\right\}^{1.93}. \quad (16)$$

Equations (16) gives the lowest limit of ρ_v/ρ_l capable of generating HP-regime for a given l/d, that is, the criterion for the onset of HP-regime.

Now, if experimental conditions, under which the occurrence of HP-regime is clearly observed, are collected from the existing data of CHF, it yields the result of Table 1 with an exceptional condition that l/d for the data of Campolunghi *et al.* [12] alone is an approximate value because of the uncertainty of tube length l corresponding to the condition of $\Delta H_i = 0$. Then, all the combinations of ρ_v/ρ_l and l/d listed in Table 1 are compared with equation (16) in Fig. 4, showing that equation (16) can predict the onset of HP-regime so far as the above data are concerned. However, equation (16) conflicts with two experimental conditions of helium I of Ogata and Sato [13, 14] shown in Fig. 4, which have been confirmed in the preceding study [4] to belong to not HP-regime but N-regime.

In Fig. 3(B), therefore, a horizontal line passing through the intersecting point P″ of equations (15) and (14) is assumed to separate HP- and N-regime, although use of equation (14) for this purpose seems to be rather unnatural from the physical point of view. The criterion for the onset of HP-regime obtained in this way is nothing but the criterion employed tentatively in the preceding study [4], and the relation between ρ_v/ρ_l and l/d at the point P″ is obtained by eliminating $\sigma\rho_l/G_2l$ from equations (15) and (14) as follows:

$$\frac{\rho_v}{\rho_l} = \left\{\frac{116(l/d)^{-0.134} + 0.976(l/d)^{0.324}}{0.254(l/d) + 82}\right\}^{1.93}. \quad (17)$$

* $C = 0.25 + \dfrac{(l/d) - 50}{150 - 50}(0.34 - 0.25)$.

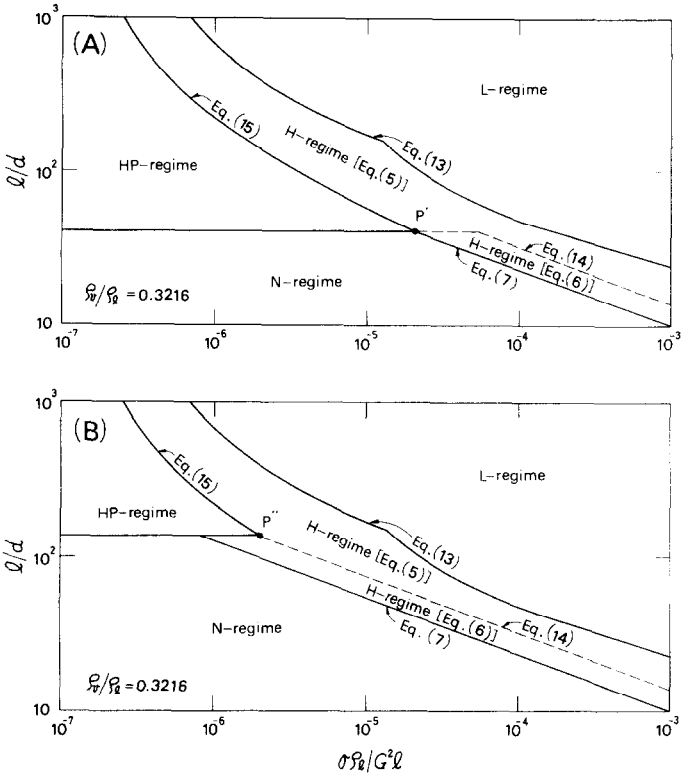

FIG. 3. Determination of the boundary between HP- and N-regime.

However, it is noted in Fig. 4 that the criterion of equation (17) for the onset of HP-regime is satisfactory for the data of helium I, but there are some discrepancies between equation (17) and the HP-regime data.

4. RE-EXAMINATION OF EXPERIMENTAL DATA OF CHF IN HP-REGIME

4.1. *New correlation of q_{co} in HP-regime*

It has been mentioned in Section 3.1 that equation (8) is considerably accurate for correlating q_{co} data. However, two questions explained in the preceding chapter seem to co-operate to suggest weaknesses of equation (8). Therefore, a careful rearrangement of equation (8) is attempted so as to improve the prediction accuracy compared with the existing data of q_{co} in HP-regime, and as the result, the following new correlation equation is obtained

Table 1. Experimental conditions generating CHF in HP-regime

Source	Experimental ranges					No. of data	Symbol
	Fluid	d (mm)	l/d	ρ_v/ρ_l	$\sigma\rho_l/G^2 l$		
Thomson–Macbeth [8]	Water	1.9	365	0.170	2.69×10^{-7}–9.15×10^{-7}	9	●
Thomson–Macbeth [8]	Water	1.9	365	0.219	1.86×10^{-7}–5.67×10^{-7}	9	□
Thomson–Macbeth [8]	Water	1.9	365	0.289	9.17×10^{-8}–3.49×10^{-7}	9	○
Peskov *et al.* [9]	Water	8.0	206	0.361	2.73×10^{-8}	1	◩
Becker *et al.* [7]	Water	10.0	200	0.140	4.83×10^{-8}–2.07×10^{-7}	8	–○–
Becker *et al.* [7]	Water	10.0	200	0.347	6.49×10^{-9}–2.40×10^{-7}	14	–●–
Becker *et al.* [7]	Water	10.0	300	0.140	3.40×10^{-8}–2.03×10^{-7}	7	△
Becker *et al.* [7]	Water	10.0	300	0.347	6.41×10^{-9}–2.61×10^{-7}	14	▲
Becker *et al.* [7]	Water	10.0	500	0.140	2.13×10^{-8}–1.28×10^{-7}	10	▽
Becker *et al.* [7]	Water	10.0	500	0.347	2.78×10^{-9}–1.32×10^{-7}	20	▼
Chojnowski–Wilson [6]	Water	32.0	238	0.243	8.43×10^{-8}–1.97×10^{-7}	3	×
Watson–Lee [10]	Water	37.8	145	0.271	4.67×10^{-8}–4.21×10^{-7}	5	■
Doroschuk *et al.* [11]	Water	8.0	188	0.201	1.50×10^{-7}	1	◐
Doroschuk *et al.* [11]	Water	8.0	188	0.271	1.76×10^{-7}–3.14×10^{-7}	2	–◐–
Campolunghi *et al.* [12]	Water	12.0	937*	0.0902–0.176			+

* An approximate value.

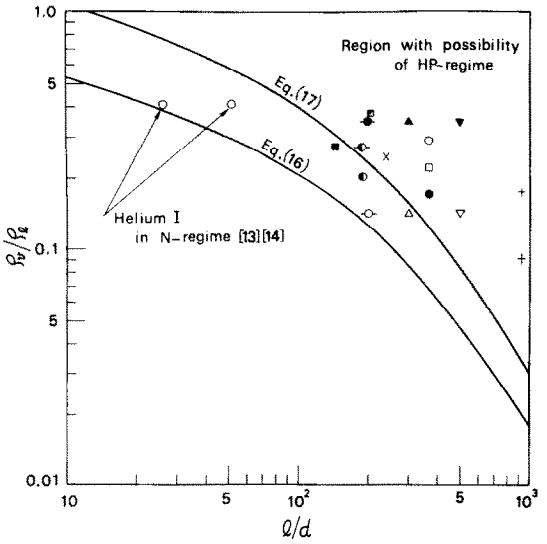

FIG. 4. Criterion for the onset of HP-regime compared with experimental data listed in Table 1.

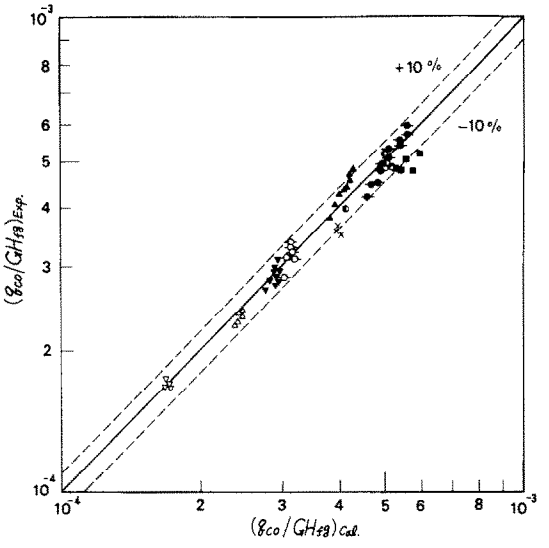

FIG. 5. Comparison of prediction of equation (8) with experimental data in HP-regime (as for the sources of data, see Table 1 through data symbols).

$$\frac{q_{co}}{GH_{fg}} = 0.0384\left(\frac{\rho_v}{\rho_l}\right)^{0.60}\left(\frac{\sigma\rho_l}{G^2 l}\right)^{0.173} \times \frac{1}{1+0.280(\sigma\rho_l/G^2 l)^{0.233}\, l/d}. \quad (18)$$

According to a comparison between equations (18) and (8) shown in the graph of $l/d = 200$ in Fig. 1, it seems in appearance as if there are no significant differences between the two equations. However, if RMS error of each equation is examined for the experimental data of q_{co} used in the study [1] to derive equation (8), it is 5.58% for equation (18) while 8.0% for equation (8), showing that equation (18) is more accurate than equation (8). Besides, if Fig. 5, which shows the comparison between the prediction of equation (18) and the experimental data, is compared with the similar result of equation (8) given in Fig. 13 of [1], it is readily found that equation (18) is superior to equation (8) in the capability of predicting q_{co} nearer the mean value of q_{co} for almost all independent series of experiment.

4.2. *New prediction equation of K for HP-regime*

If equation (18) is adopted instead of equation (8), new theoretical prediction of K in HP-regime is given by the following equation instead of equation (12) (cf. [3] for the derivation process):

$$K_{HP} = 1.12\frac{1.52(\sigma\rho_l/G^2 l)^{0.233} + d/l}{(\rho_v/\rho_l)^{0.60}(\sigma\rho_l/G^2 l)^{0.173}}. \quad (19)$$

Then, in Fig. 6, K_{HP} predicted by equation (19) is compared with the same experimental data of K_{HP} as used in Fig. 2, showing a marked improvement of accuracy in predicting K_{HP} as compared with Fig. 2.

4.3. *Criterion for the onset of HP-regime*

Eliminating q_{co} from equations (5) and (18), it yields the following equation for the boundary between H- and HP-regime:

$$\frac{l}{d} = \frac{0.384(\rho_v/\rho_l)^{0.467} - (\sigma\rho_l/G^2 l)^{0.160}}{0.280(\sigma\rho_l/G^2 l)^{0.393} - 0.00119(\rho_v/\rho_l)^{0.467}}. \quad (20)$$

Then, if equation (20) is used instead of equation (15), Fig. 3(A) is replaced by Fig. 7, where a horizontal line passing through the intersecting point P of equations (20) and (7) separates HP- and N-regime, and the relation between ρ_v/ρ_l and l/d at the point P is obtained by eliminating $\sigma\rho_l/G^2 l$ from equations (20) and (7) as follows:

$$\frac{\rho_v}{\rho_l} = \left\{\frac{89.3(l/d)^{-0.432} + 21.2(l/d)^{-0.062}}{0.119(l/d) + 38.4}\right\}^{2.14}. \quad (21)$$

In Fig. 8, equation (21) is compared with the same experimental data as those in Fig. 4, leading to the conclusion that equation (21) can be a criterion for the onset of HP-regime satisfying all the experimental data shown in Fig. 8.

Lines of constant $\sigma\rho_l/G^2 l$ drawn in the region of generating HP-regime in Fig. 8 are given by equation (20), indicating the highest limit of $\sigma\rho_l/G^2 l$ which enables the appearance of HP-regime at a given point $(\rho_v/\rho_l,\ l/d)$ in Fig. 8. Among the experimental data listed in Table 1, data of Thomson and Macbeth [8] for $l/d = 365$ and $\rho_v/\rho_l = 0.170$ (denoted by ● in Fig. 8) alone are in the experimental range of $\sigma\rho_l/G^2 l$ which is somewhat higher than the limiting value indicated in Fig. 8. However, if the above data are examined carefully, it reveals that there is the possibility of

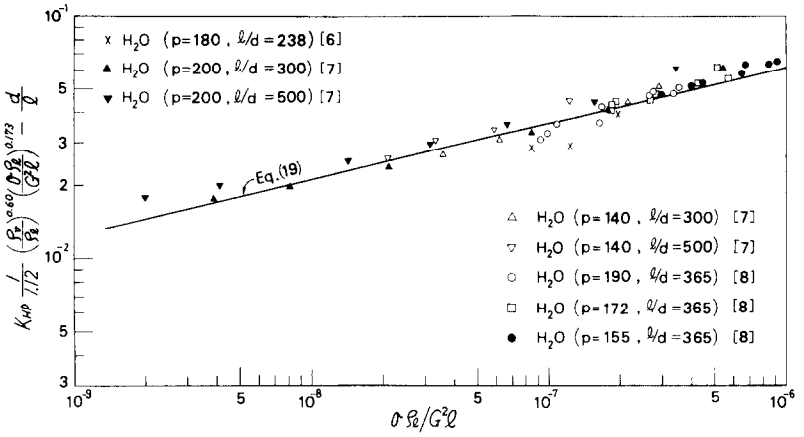

FIG. 6. Comparison between prediction of equation (19) and experimental data for K_{HP}.

retaining the transition character between H- and HP-regime, accordingly the slight deviation such as mentioned above may not be regarded as a serious matter. *Supplementary note.* Two data of helium I shown in Fig. 8 are those obtained under the following conditions of $\sigma\rho_l/G^2l$ respectively: $\sigma\rho_l/G^2l = 5.70 \times 10^{-6}$ for the data of $l/d = 25.7$, and $\sigma\rho_l/G^2l = 2.90 \times 10^{-6}$ for that of $l/d = 51.4$.

5. CHF-REGIME MAP

Experiments of CHF made so far in HP-regime are not necessarily sufficient in number as is noticed in Fig. 8. In addition, the existing experimental data for HP-regime are limited to only one fluid, that is water (cf. Table 1). Therefore, further experimental studies of wide range may be necessary in order to give the final approval on the criterion of Fig. 8 for the onset of HP-regime.

However, the criterion mentioned above is regarded as most reliable at the present stage at least. In other words, the means represented by Fig. 7 is most suitable at present for making CHF-regime map. Accordingly, employing the method of Fig. 7, the CHF-regime map is made for each condition of $\rho_v/\rho_l = 0.01787, 0.04847, 0.1351$, and 0.3216 (which corresponds to the pressure $p = 29.5, 69, 137$ and 196 bar in case of water) to give the result of Fig. 9. In every regime illustrated in Fig. 9, the correlation equation of q_{co} that is applicable in the regime is shown together with the prediction equation of K except N-regime, for which the prediction equation of K has not been determined due to non-linear q_c–ΔH_i relationship [1–3]. In addition, a vertical broken line indicated on the upper right side of each diagram of Fig. 9 represents the position of $\sigma\rho_l/G^2l = 7.84 \times 10^{-4}$, which corresponds to the intersecting point of equations (3) and (4) such as shown in the graph of $l/d = 200$ in Fig. 1.

In sum, CHF-regime map of Fig. 9 is a revision of the CHF-regime map proposed in the author's first report (that is Fig. 15 of [1]), taking into account the results obtained in the subsequent studies.

6. CONCLUSIONS

(i) Regarding generalized correlation equations of CHF of forced convection boiling in uniformly heated vertical tubes, the results obtained in the author's

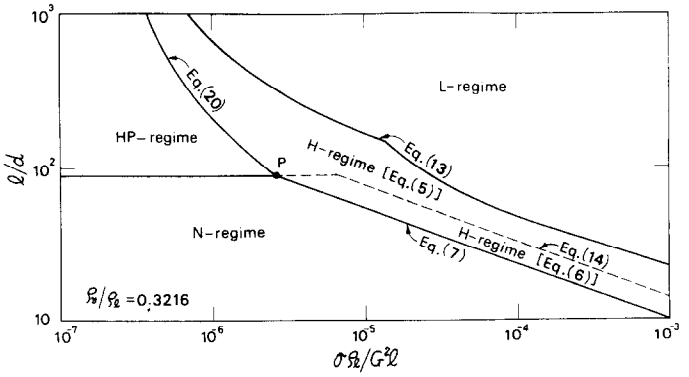

FIG. 7. New method for determining the boundary between HP- and N-regime.

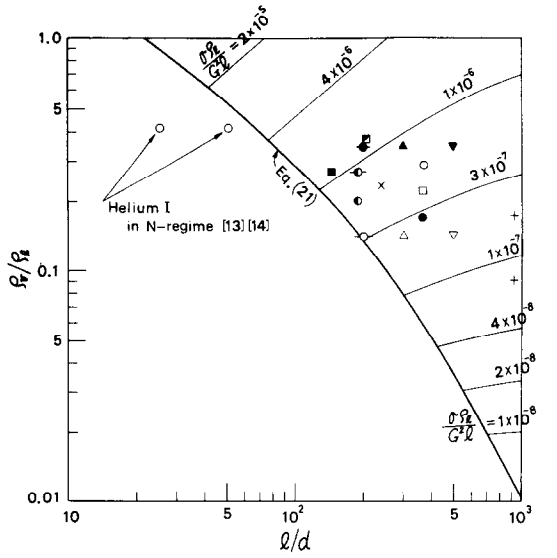

FIG. 8. New criterion for the onset of HP-regime compared with experimental data listed in Table 1.

previous papers [1–4] are summarized in equations (3)–(12) of this paper.

(ii) Through re-examination of existing experimental data of CHF in HP-regime, it is found that equation (8) for the correlation of q_{co} should be replaced by new equation (18), and similarly, equation (12) for the parameter K_{HP} by new equation (19), equation (15) for the boundary between H- and HP-regime by new equation (20), and equation (16) or (17) for the onset of HP-regime by new equation (21). Comparisons of these new equations with experimental data are shown in Figs. 5, 6 and 8.

(iii) A CHF-regime map for forced convection boiling in uniformly heated tubes is determined as shown in Fig. 9, taking into account all the informations obtained so far in the author's studies.

Acknowledgements—The Ministry of Education, Science and Culture is acknowledged for the financial support to this study under Grant in Aid of Special Project Research No. 411002 (1979).

REFERENCES

1. Y. Katto, A generalized correlation of critical heat flux for the forced convection boiling in vertical uniformly heated tubes, *Int. J. Heat Mass Transfer* **21**, 1527–1542 (1978).
2. Y. Katto, A generalized correlation of critical heat flux for the forced convection boiling in vertical uniformly heated tubes—a supplementary report, *Int. J. Heat Mass Transfer* **22**, 783–794 (1979).
3. Y. Katto, An analysis of the effect of inlet subcooling on critical heat flux of forced convection boiling in vertical uniformly heated tubes, *Int. J. Heat Mass Transfer* **22**, 1567–1575 (1979).
4. Y. Katto, General features of CHF of forced convection boiling in uniformly heated vertical tubes with zero inlet subcooling, *Int. J. Heat Mass Transfer* **23**, 493–504 (1980).

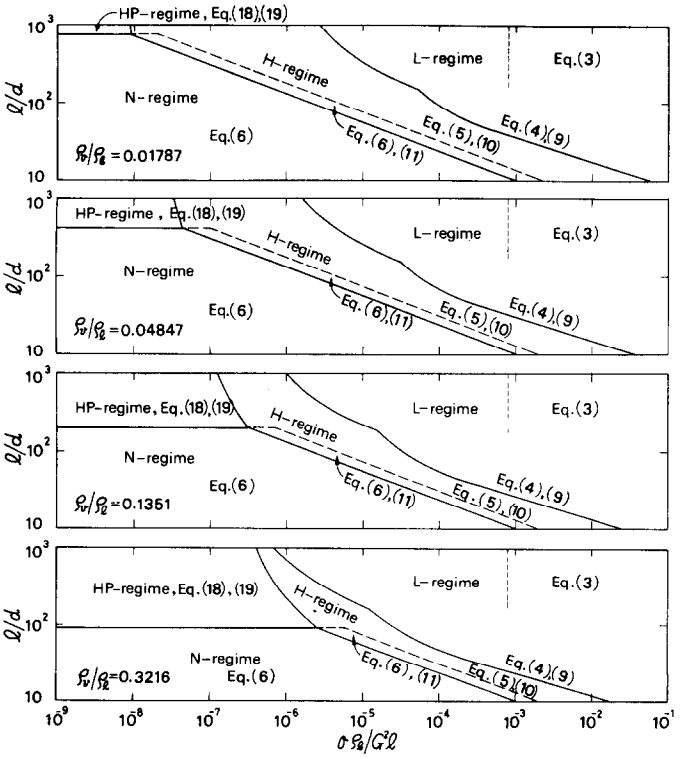

FIG. 9. CHF-regime map with the indication of correlation equations of CHF in each regime (see Fig. 7 for the determination of boundaries of each regime).

5. J. G. Collier, *Convective Boiling and Condensation*, p. 240. McGraw-Hill, New York (1972).
6. B. Chojnowski and P. W. Wilson, Critical heat flux for large diameter steam generating tubes with circumferentially variable and uniform heating, in *Heat Transfer 1974*, Vol. IV, pp. 260–264. Hemisphere, Washington (1974).
7. K. M. Becker, D. Djursing, K. Lindberg, O. Eklind and C. Österdahl, Burnout conditions for round tubes at elevated pressures, in *Progress in Heat and Mass Transfer*, Vol. 6, pp. 55–74. Pergamon Press, Oxford (1972).
8. B. Thompson and R. V. Macbeth, Boiling water heat transfer burnout in uniformly heated round tubes: a compilation of world data with accurate correlations, UKAEA, AEEW-R 356 (1964).
9. O. L. Peskov, V. I. Subbotin, B. A. Zenkevich and N. D. Sergeyev, The critical heat flux for the flow of steam–water mixtures through pipes, in *Problems of Heat Transfer and Hydraulics of Two-Phase Media* (edited by S. S. Kutateladze), pp. 48–62. Pergamon Press, Oxford (1969).
10. G. B. Watson and R. A. Lee, Critical heat flux in inclined and vertical smooth and ribbed tubes, in *Heat Transfer 1974*, Vol. IV, pp. 275–279. Hemisphere, Washington (1974).
11. V. E. Doroschuk, L. L. Levitan and F. P. Lantzman, Investigation into burnout in uniformly heated tubes, ASME-Paper, No. 75-WA/HT-22 (1975).
12. F. Campolunghi, M. Cumo, G. Ferrari, R. Leo and G. Vaccaro, Burn-out power in once-through tubular system generators, in *Heat Transfer 1974*, Vol. IV, pp. 280–284. Hemisphere, Washington (1974).
13. H. Ogata and S. Sato, Critical heat flux for two-phase flow of helium I, *Cryogenics* **13**, 610–611 (1976).
14. H. Ogata, Private communication.

FLUX DE CHALEUR CRITIQUE EN EBULLITION AVEC CONVECTION FORCEE DANS DES TUBES VERTICAUX UNIFORMEMENT CHAUFFES (FORMULATION DU CHF EN REGIME HP ET DETERMINATION DU GRAPHE DES REGIMES CHF)

Résumé—Les précédentes études de l'auteur sur la formulation générale du flux de chaleur critique (CHF) dans les tubes sont prolongées par un nouvel examen des données expérimentales du CHF en régime de haute pression (HP) pour obtenir de nouvelles équations plus précises. D'autre part le critère d'apparition du CHF dans ce régime HP est révisé de façon à satisfaire toutes les données expérimentales connues et ainsi un graphe mieux défini des régimes caractéristiques de CHF dans les tubes chauffés est déterminé.

KRITISCHE WÄRMESTROMDICHTE (KWD) BEIM STRÖMUNGSSIEDEN IN GLEICHMÄSSIG BEHEIZTEN SENKRECHTEN ROHREN (KORRELATION DER KWD IM HOCHDRUCKGEBIET UND AUFSTELLUNG EINER KWD-BEREICHSKARTE)

Zusammenfassung — Wegen der Konfrontation mit zwei wichtigen Fragen, die von den früheren Untersuchungen des Autors über die verallgemeinerte Korrelation der KWD in Rohren herrühren, wurden die experimentellen Daten der KWD im Hochdruckbereich erneut untersucht, um neue Gleichungen mit größerer Genauigkeit für die KWD in diesem Gebiet zu erhalten. Das Kriterium für den Beginn der KWD im Hochdruckgebiet konnte ebenfalls revidiert werden, so daß Übereinstimmung mit allen existierenden experimentellen Daten erreicht wurde. Schließlich wurde eine Karte mit eindeutig bestimmten charakteristischen Bereichen der KWD in gleichmäßig beheizten Rohren aufgestellt.

КРИТИЧЕСКИЙ ТЕПЛОВОЙ ПОТОК ПРИ КИПЕНИИ В УСЛОВИЯХ ВЫНУЖДЕННОЙ КОНВЕКЦИИ В РАВНОМЕРНО НАГРЕВАЕМЫХ ВЕРТИКАЛЬНЫХ ТРУБАХ (КОРРЕЛЯЦИЯ КРИТИЧЕСКОГО ТЕПЛОВОГО ПОТОКА В РЕЖИМЕ ВЫСОКОГО ДАВЛЕНИЯ И СОСТАВЛЕНИЕ КАРТЫ РЕЖИМОВ КРИТИЧЕСКОГО ТЕПЛОВОГО ПОТОКА)

Аннотация — При использовании предложенного ранее автором соотношения для критического теплового потока (КТП) возникло два важных вопроса. Поэтому были пересмотрены экспериментальные данные по КТП в режиме высокого давления с целью получения более точных соотношений для КТП в данном режиме. Уточнен также критерий, определяющий наступление КТП в режиме высокого давления, который удовлетворяет всем имеющимся экспериментальным данным, и, наконец, составлена карта режимов КТП в разномерно нагреваемых трубах.